Bioelectrochemistry 147 (2022) 108215

Contents lists available at ScienceDirect

Bioelectrochemistry

journal homepage: www.journals.elsevier.com/bioelectrochemistry

Improvement of laccase biosensor characteristics using sulfur-doped TiO_2 nanoparticles

Taras Kavetskyy [a,b,*], Oleh Smutok [c,*], Olha Demkiv [a,d], Yuliia Kukhazh [a], Nataliya Stasyuk [a,d], Evhen Leonenko [e], Arnold Kiv [f,g], Yoshinori Kobayashi [h], Atsushi Kinomura [i], Ondrej Šauša [j,k], Mykhailo Gonchar [a,d], Evgeny Katz [c,*]

[a] Drohobych Ivan Franko State Pedagogical University, Drohobych 82100, Ukraine
[b] The John Paul II Catholic University of Lublin, Lublin 20-950, Poland
[c] Department of Chemistry & Biomolecular Science, Clarkson University, Potsdam, NY 13699-5810, USA
[d] Institute of Cell Biology, National Academy of Sciences of Ukraine, Lviv 79005, Ukraine
[e] L.V. Pisarzhevskii Institute of Physical Chemistry National Academy of Sciences of Ukraine, Kyiv 03028, Ukraine
[f] Ben-Gurion University of the Negev, Beer-Sheva 84105, Israel
[g] South-Ukrainian K.D. Ushynsky National Pedagogical University, Odesa 65020, Ukraine
[h] Waseda Research Institute for Science and Engineering, Waseda University, Tokyo 169-8050, Japan
[i] Institute for Integrated Radiation and Nuclear Science, Kyoto University (KURNS), Kumatori, Osaka 590-0494, Japan
[j] Department of Nuclear Chemistry, Comenius University in Bratislava, Bratislava 84215, Slovakia
[k] Institute of Physics, Slovak Academy of Sciences, Bratislava 84511, Slovakia

ARTICLE INFO

Dedicated to celebrating Frieders Scheller 80th Birthday in 2022.

Keywords:
Sulfur-doped TiO_2
Nanoparticles
Nafion membrane
Laccase
Amperometric biosensor

ABSTRACT

The search for new nanoscale materials with predictable properties to target the timely and fast detection of toxic components in wastewater is one of the most promising directions of modern biosensorics. We have shown that TiO_2 nanoparticles modified with sulfur significantly improve the main operational parameters of laccase-based electrodes when compared with controls. The nanoparticle samples were labeled as TiO_2S(0.75), TiO_2S(1.5), and TiO_2S(3.0), in which the numbers in parentheses refer to the quantity of H_2SO_4 (mL) used in the synthesis. The nanoparticles and enzyme were immobilized by means of Nafion film formed on a carbon rod electrode. It was shown that the modification of Nafion film by TiO_2 or TiO_2S(1.5) nanoparticles does not affect the size of the nanocavities and defect structure of the main polymer matrix as revealed by positron annihilation spectroscopy. It testifies that the structural-morphological difference between the film samples is rather small, and the improving of the sensor operational parameters for TiO_2S(1.5)-based laccase electrodes is connected only with the impact of sulfur doping, but not the difference in membrane properties. The developed bioelectrodes were tested for phenol analysis in real communal wastewater samples spiked with these analytes, demonstrating the high accuracy of the assay.

1. Introduction

Recently, new nanoparticles with unique properties have been widely used to create amperometric biosensors with improved performance characteristics [1,2,3]. A wide range of such nanoparticles has been obtained using carbon [4,5,6] or its complexes with metals [7,8], as well as using metals, such as iron [9], noble metals [10,11], and transition elements [12,13,14,15]. Among the transition metals and their compounds, much attention has been paid to titanium dioxide (TiO_2) [16]. This is an inexpensive semiconductor material with a high surface reactivity, in particular, to the adsorption of biomolecules [17]. Its properties make it possible to significantly improve the kinetics of electron transfer in bio-nanomembranes of amperometric laccase-based biosensors [18,19,20]. The optimization of the co-immobilization procedure for laccase and nanoparticles to exhibit a maximum of the enzymatic activity in the sensor's microenvironment, simultaneously ensuring good diffusional properties of the formed bionanocomposite membrane, is a critical point in such biosensors' construction. In this

* Corresponding authors at: Drohobych Ivan Franko State Pedagogical University, 24 I. Franko Str., Drohobych 82100, Ukraine. (T. Kavetskyy). Department of Chemistry & Biomolecular Science, Clarkson University, 8 Clarkson Avenue, Box 5810, Potsdam, New York 13699-5810, USA. (O. Smutok, E. Katz).
E-mail addresses: kavetskyy@yahoo.com (T. Kavetskyy), osmutok@clarkson.edu (O. Smutok), ekatz@clarkson.edu (E. Katz).

https://doi.org/10.1016/j.bioelechem.2022.108215
Received 19 April 2022; Received in revised form 15 July 2022; Accepted 20 July 2022
Available online 25 July 2022

point of view, the physical entrapment with highly permeable membranes looks to be very promising among the known immobilization techniques due to its simplicity and a minimal effect on the structural and conformational changes of the incorporated/held bio-nano molecules [21].

In this work, we considered the possibility of using sulfur-doped TiO_2 to create an efficient laccase-based amperometric biosensor. The work was undertaken in connection with the unusual acid-base properties of this material [22] and the unique properties of the laccase. The laccases from *Trametes* are characterized with five conserved cysteine residues (amino acid contains a thiol group) in the enzyme sequences. Three of them are in the middle and two in the *C*-terminal of the sequences. It indicates that the cysteine residues have a functional role in forming intermolecular and intramolecular disulfide bonds for these laccases [23]. The sulfur in sulfur doped TiO_2 is able to form disulfide bonds with cysteine residues of laccase affected on enzyme structure and its intramolecular interactions, affecting on the kinetic properties of the formed bio-nanocomposite. This hypothesis is supported with our results indicated an increasing affinity toward ABTS and catechol in twice for the bioelectrodes based on $TiO_2S(1.5)$ compared to the control bioelectrodes based on single laccase. Moreover, the disulfide bonds between TiO_2S and external cysteine residues of the enzyme additionally support non-covalent immobilization of the protein in the bio-nanocomposite layer of the sensor membrane. This dual effect of sulfur of TiO_2S could significantly improve of the operational parameters of the biosensor. In the course of the work, we revealed an effective non-covalent immobilization of the enzyme into the nanolayer of the biosensor membrane. To enhance this immobilization effect, the sulfur-containing Nafion polymer was used, which additionally retains the sulfur-containing components of the bio-nano-membrane and ensures its higher stability. The resulting nanomaterials were characterized by physicochemical methods, and the optimized bio-nano-modified electrodes were approbated to accurate phenol analysis in real communal wastewater spiked with these analytes.

2. Experimental details

2.1. Materials

Laccase enzyme (E.C. 1.10.3.2) from *Trametes versicolor* with activity of $\geq$ 10 U·mg^{-1}, 2,2′-azino-*bis*(3-ethylbenzthiazoline-6-sulfonic acid) (ABTS), 99%, catechol, phenol, Nafion®, and other reagents and buffer compounds were purchased from Sigma-Aldrich (Darmstadt, Germany). AEROXIDE®TiO2 P25 (average diameter 25.4 nm; specific surface area (BET) 35–65 m^2/g; composition: 90 wt% anatase and 10 wt% rutile) was obtained from (Evonik industries AG, Essen, Germany). All chemicals and reagents were prepared using triple distilled water. Prior to analysis, the raw wastewater sample was filtered through a Millipore 0.45 μm filter.

2.2. Preparation of sulfur-doped TiO_2 nanoparticles

The TiO_2 samples were prepared by controlled hydrolysis of titanium butoxide, followed by hydrothermal treatment according to a modified method [24]. In a typical synthesis, 20 mL acetic acid was added dropwise to a flask containing 10 mL titanium butoxide, diluted in 30 mL absolute ethanol, followed by the addition of 0.75–3.0 mL H_2SO_4 (total concentration H_2SO_4 0.2–1.0 mol·L^{-1}). The obtained clear solution was sonicated at 40 °C for 1 h and at 60 °C for 3 h, resulting in the formation of a sol, which was further transferred into a stainless autoclave and kept at 120 °C for 12 h. The precipitates were separated, washed thoroughly several times, dried in air at 100 °C for 24 h, and calcined at 375 °C for 2 h. The nanoparticles samples were labeled as $TiO_2S(0.75)$, $TiO_2S(1.5)$, and $TiO_2S(3.0)$, in which the numbers in parentheses refer to the quantity of H_2SO_4 (mL) used in the synthesis.

2.3. Energy dispersive X-ray spectroscopy and scanning electron microscopy

The X-ray diffraction pattern was recorded on a Bruker D8 Advance diffractometer. The morphology of the obtained sample was studied using a JCM-5000 scanning electron microscope. A rigorous quantitative elemental microanalysis was performed by SEM/EDX following the k-ratio/matrix correction protocol.

2.4. Positron annihilation spectroscopy

Doppler broadening of annihilation radiation (DBAR) and positron annihilation lifetime spectroscopy (PALS) measurements were performed using a monoenergetic slow positron beam generated by the Kyoto University Research Reactor. Line-shape parameters (*S* parameters) as a function of energy in the range of 0–25 keV were obtained in the DBAR measurements to confirm the sample thickness. After that, an optimum energy for PALS measurements was determined to be 3 keV, corresponding to the middle of the film. PALS spectra of a polyimide (Kapton) film were measured as a standard, as well as the sample spectra. Detailed descriptions of the slow-positron measurement system can be found elsewhere [25].

2.5. Formation of bio-nanocomposite membrane of the biosensor

The formation of bio-nanocomposite membrane of the biosensor was performed as follows. 10 μL of enzyme solution (with a concentration of 1 mg·mL^{-1} and a volumetric activity of 13.6 U·mL^{-1}, in 50 mm acetate buffer, pH 4.5) was mixed with 5 μL of a colloidal solution of TiO_2S (sulfur dopant content) particles (1 mg·mL^{-1}) in 1 % aqueous solution of Nafion. The formed mixture was dropped onto the 3.05 mm diameter carbon rod working electrode, with the next step of drying the resulting mixture (nanoparticles + enzyme + polymer) for 10 min occurring in air at room temperature. After drying, mechanically strong TiO_2S-enzyme-Nafion biocomposite membrane was formed on the surface of the carbon rod electrode. The prepared bio-nanofunctionalized electrodes were rinsed with 50 mM acetate buffer, pH 4.5 and kept at 4 °C till usage.

2.6. Construction of amperometric biosensor

The amperometric biosensors were constructed in a three-electrode configuration to be used for constant-potential amperometry. The biosensor configuration included a Pt counter electrode, Ag/AgCl/KCl (3 M) reference electrode, and a graphite-rod (type RW001, 3.05 mm) from Ringsdorff Werke (Bonn, Germany) as a working electrode. Before usage, the working electrodes were polished with P2000 emery paper. The amperometric analysis was carried out using a potentiostat CHI 1200A (IJ Cambria Scientific, Burry Port, UK) in an electrochemical cell at room temperature, avoiding direct light and under continuous stirring .

The amperometric measurements were performed in a glass electrochemical cell with a working volume of 50 mL, filled with 20 mL acetate buffer, pH 4.5 at room temperature, avoiding direct light. For cyclic voltamperometry, operational conditions were as follows: scanning rate 7 mV·s^{-1} *vs* Ag/AgCl/KCl(3 M) reference electrode in 50 mM acetate buffer, pH 4.5 at room temperature. For chronoamperometric analysis, the bio-nano-modified electrodes were placed in a vigorously stirred solution and, after setting the base signal at an operating potential of −150 mV *vs* Ag/AgCl, increasing aliquotes of laccase substrate (ABTS, catechol or phenol) were added to the measuring cell.

3. Results and discussion

3.1. Characterization of sulfur-doped TiO_2 nanoparticles

The X-ray diffraction spectra of TiO_2S (sulfur dopant content)

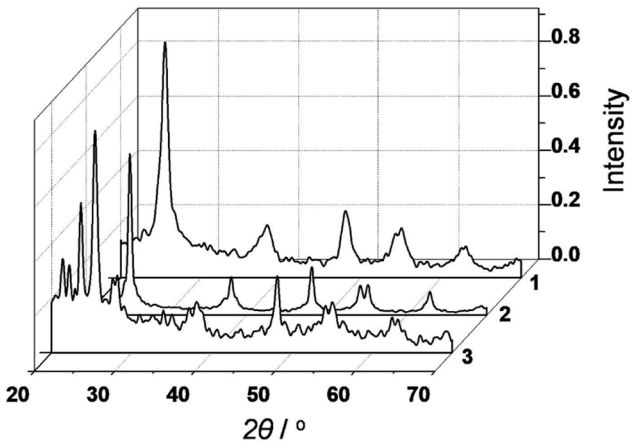

Fig. 1. XRD spectra of TiO_2S samples with different content of dopant in the reaction mixture: 1 – TiO_2S(0.75); 2 – TiO_2S(1.5); 3 – TiO_2S(3.0).

samples as a function of the concentration of sulfuric acid are presented in Fig. 1. As seen from this figure, under the selected synthesis conditions, decrease (TiO_2S(0.75), curve 1) or increase (TiO_2S(3.0), curve 3) of the concentration of the doping agent leads to the formation of different phases. A decreased doping agent concentration resulted in the presence of only motives of crystal structure (anatase), which are characterized by the presence of the signals corresponding to reflections from the planes of anatase phase at 25.24° (101), 36.98° (004), 48.02° (200) and 62.74° (204), while a mixture of anatase/titanyl sulfate phases is observed in the sample with the maximum dopant concentration [26]. Thus, the concentration of dopant can be a determining factor of the crystallinity and different crystal phases of the obtained structures.

The results of SEM/EDX analysis of the corresponding TiO_2S samples are presented in Fig. 2 and Table S1 and Figs. S1, S2 (*Supplementary material*). The formation of almost monodisperse spheres of regular shape with a diameter of about 100 nm and 500 nm is characteristic of the samples TiO_2S(0.75) (Fig. 2, A) and TiO_2S(1.5) (Fig. 2, B), respectively. The synthesized samples with a higher concentration of sulfuric acid TiO_2S(3.0) are polydisperse materials with indeterminate morphology, with hierarchical particle distribution and the appearance of aggregated domains (Fig. 2, C).

All obtained TiO_2S samples were tested for their ability for efficient electronic exchange in the biorecognition layer of the amperometric biosensors based on laccase-entrapped with Nafion membrane. Typical SEM images of Nafion/TiO_2S(1.5) composite membrane are shown in Fig. S3 (*Supplementary material*). It is seen that TiO_2S(1.5) nanoparticles with a size of about 500 nm are evenly distributed in the Nafion matrix.

According to the obtained EDX results and calculations (*Supplementary material* Table S1), the concentration of sulfur in the spheres can be estimated as 2.4 ± 0.2%, 6.0 ± 0.3%, and 12.0 ± 0.8% by weight for TiO_2S(0.75), TiO_2S(1.5), and TiO_2S(3.0) samples, respectively. It should be noted that with increasing concentration of sulfur in the TiO_2S(3.0) sample there is a deviation from the stoichiometric number of oxygen and titanium atoms in the classical TiO_2 structures.

3.2. Characterization of Nafion-formed films

The possible structural-morphological difference between polymer matrices of the Nafion formed films: Nafion itself, Nafion with commercial TiO_2 (Nafion/AEROXIDE®TiO2 P25), and Nafion with TiO_2S (1.5) (Nafion/TiO_2S(1.5)) were examined using positron annihilation spectroscopy (PAS). The samples were tested in the form of thin films onto a glass support. To characterize the obtained composites, the PAS method using a slow positron beam with variable energy, known as variable-energy slow positron beam, was used as developed at the Institute of Integrated Radiation and Nuclear Science (KURNS), Kyoto University (Japan).

The positron pulse system of the slow positron beam in KURNS is designed as a PAS variant for the study of thin films or near-surface layers. It has been confirmed that the pulse system is effective for samples with relatively short positron life ($\tau < 1$ ns), in the case of metals and semiconductors without *ortho*-positronium (*o*-Ps) formation. In this study, we confirmed the suitability of the slow positron beam system for the studied polymer samples with the *o*-Ps component.

Initially, the DBAR method was used to obtain the penetration depth profile of positrons in the studied polymer films (*Supplementary material* Fig. S4). It was found that at a positron energy of 3 keV, the annihilation of positrons occurs right in the middle of the polymer matrix (a

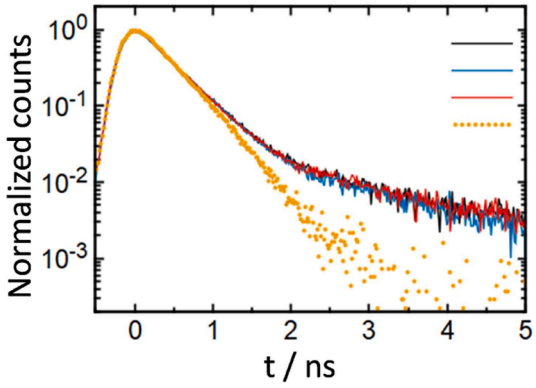

Fig. 3. The positron annihilation lifetime (PAL) spectra at positron energy of 3 keV for the studied polymer films: Nafion (black), Nafion/AEROXIDE®TiO2 P25 (blue), Nafion/TiO_2S(1.5) (red), Kapton (orange). The PAL spectrum of Kapton foil without *o*-Ps component is shown for comparison.

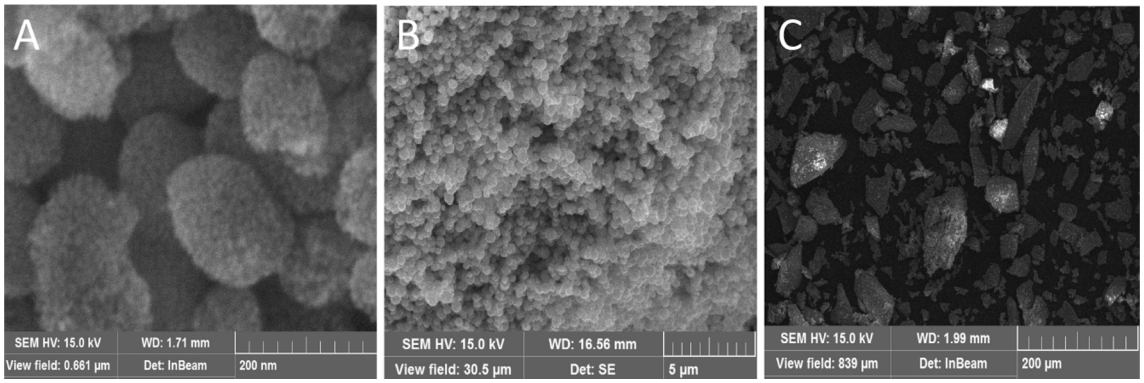

Fig. 2. SEM images of TiO_2S samples with different content of dopant in the reaction mixture: A – TiO_2S(0.75); B – TiO_2S(1.5); C – TiO_2S(3.0).

Table 1
Positron annihilation lifetimes and intensities of *o*-Ps at incident positron energy of 3.0 keV and calculated radius of holes for the studied polymer films: Nafion, Nafion/AEROXIDE®TiO2 P25 and Nafion/TiO_2S(1.5).

Sample	$\tau_{o\text{-Ps}}$, ns	$I_{o\text{-Ps}}$, %	R_h, nm
Nafion	2.2415 ± 0.0758	9.4359 ± 0.2305	0.307
Nafion/AEROXIDE®TiO2 P25	2.2548 ± 0.0825	8.1045 ± 0.2023	0.308
Nafion/TiO_2S(1.5)	2.2562 ± 0.0714	9.3406 ± 0.1974	0.308

minimum on the plot of *S*-parameter *vs* positron energy E_p).

The lifetime spectra in the PAS method at a positron energy of 3 keV for the studied samples of polymer films Nafion, Nafion/AEROXIDE®TiO2 P25 and Nafion/TiO_2S(1.5) are shown in Fig. 3. Table 1 shows the obtained values of the *o*-Ps, i.e. lifetime, $\tau_{o\text{-Ps}}$, and intensity, $I_{o\text{-Ps}}$. The radius of free-volume nanocavities or holes, R_h, was calculated based on the Tao-Eldrup equation [27,28].

$$\tau_{o-Ps} = 0.5\left[1 - (R_h/(R_h + \Delta R)) + (2\pi)^{-1} sin(2\pi R_h/(R_h + \Delta R))\right]^{-1} \quad (1)$$

Here, $\Delta R = 0.1656$ nm is an empirical parameter [29]. This value is accepted for a wide range of materials. In our case, the presence of the *o*-Ps component with a lifetime in the region of ns was found. It is seen that the presence of AEROXIDE®TiO2 P25 or TiO_2S(1.5) nanoparticles in the volume of Nafion does not affect the *o*-Ps lifetime in the range of experimental errors. This may mean that positronium formation predominates in the Nafion volume, whose cavities are not affected by the TiO_2 material. At the same time, the presence of TiO_2 nanoparticles in the investigated sample material suppresses the formation of Ps. Implanted positrons in the environment of nanoparticles predominantly annihilate with electrons directly, without the formation of Ps. It is known from the literature that for denser TiO_2 structures the Ps formation is strongly reduced [30]. This could explain the decrease in the intensity $I_{o\text{-Ps}}$ for TiO_2-containing material. As shown in Table 1, the presence of sulfur mitigates the effect of suppressing Ps formation. It is seen that the modification of the Nafion film by AEROXIDE®TiO2 P25 and TiO_2S(1.5) nanoparticles does not affect the size of the nanocavities and the intensity of *o*-Ps in the presence of sulfur. The same *S*-E_p trends obtained by the DBAR method (*Supplementary material* Fig. S4) also show that the defect structure of these samples does not differ.

The information obtained from the PAS method on the similarity of defect structure and free-volume nanocavities in the Nafion polymer matrix with and without S-doped TiO_2 nanoparticles is important for understanding the mechanism of the immobilization of enzyme using these polymer materials in the construction of amperometric biosensors. It testifies that the structural-morphological difference between the film samples is rather small and that improving the sensor operational parameters for TiO_2S(1.5)-based laccase electrodes is connected only with the impact of sulfur doping, and not the difference in the membrane properties.

3.3. Construction and evaluation of laccase-based biosensor using sulfur-doped TiO_2 nanoparticles (TiO_2S)

To form the bionanorecognizing layer of the biosensor on the surface of solid transducers (working electrodes), it is necessary to fix all components of the bio-recognizing film (TiO_2S and enzyme) while maintaining their electrochemical and catalytic properties. For this purpose, Nafion was used. Nafion is a synthetic polymer based on tetrafluoroethylene with ionic properties. The unique ionic properties of Nafion are the result of the inclusion of perfluorovinyl ether groups ending with sulfonate groups based on tetrafluoroethylene (*Supplementary material* Fig. S5).

The commercial laccase (EC 1.10.3.2 *p*-diphenol:oxygen oxidoreductase from *Trametes versicolor*), a copper-containing enzyme, was used for the biosensor construction. In a typical laccase reaction, the phenolic substrate is subjected to one-electron oxidation to form an aryl radical, which in the next stage of the enzymatic reaction is converted to quinone. The operation of the laccase-based amperometric biosensor is based on the reduction of the oxidized products generated by the laccase-catalyzed reaction, which correspond to the following transformations: for ABTS → cation radicals $ABTS^{+\bullet}$ or $ABTS^{(2+\bullet)}$, and for catechol → semiquinone intermediate → semiquinone (*Supplementary material* Fig. S6).

The cyclic voltamperometric analysis using ABTS as a model laccase substrate was performed to estimate the optimal working potential of the reduction of electroactive products of the laccase's reaction with a bioelectrode based on Nafion/TiO_2S bio-nanocomposite membrane (*see supplementary material* Fig. S7). It has been shown that the addition of ABTS to the measuring cell resulted in an increase in the cathodic currents of the bio-nano-modified electrode. The significant increase in the currents clearly indicates the high efficiency of electron transfer between the electroactive product of the laccase reaction and the Nafion/TiO_2S-modified surface of the working electrode. In addition, it allows for estimation of the optimal operating potential for the biosensor, which corresponds to −150 mV *vs* Ag/AgCl/KCl(3 M) reference electrode. The same working potential is commonly used for numerous developed catechol and phenol sensitive biosensors [4,31,32]. Such relatively low operating potential makes the biosensor more selective, avoiding the interfering response of electroactive chemicals, contained in real samples, which can be auto-oxidized or auto-reduced at extreme operating potential values. That is why the potential of −150 mV *vs* Ag/

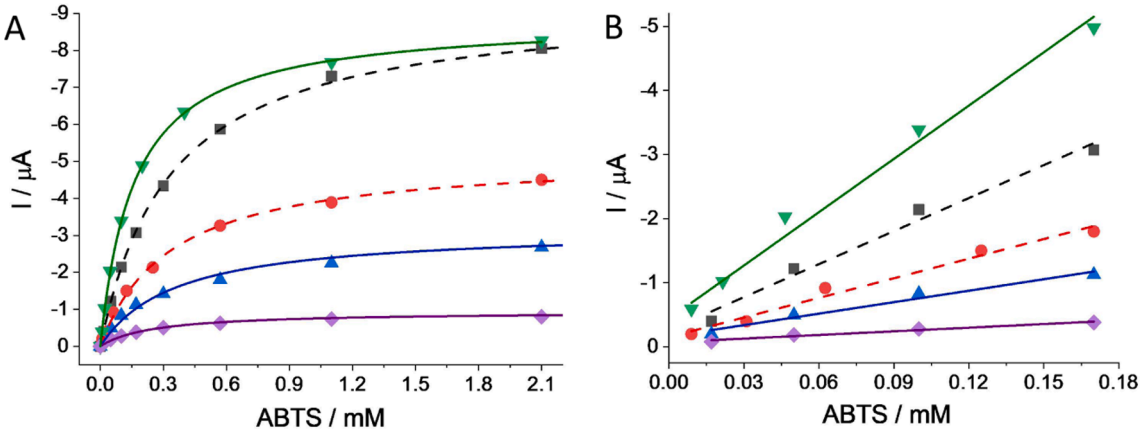

Fig. 4. Typical chronoamperometric calibration curves of bioelectrodes response for substrate saturation (A) and within the linear range (B) toward subsequent addition of increasing ABTS concentration. Solid lines – bioelectrodes based on TiO_2S: TiO_2S(0.75) (blue), TiO_2S(1.5) (green), and TiO_2S(3.0) (violet); dash lines – control bioelectrodes: without of TiO_2 (red) and based on commercial AEROXIDE®TiO2 P25 (black).

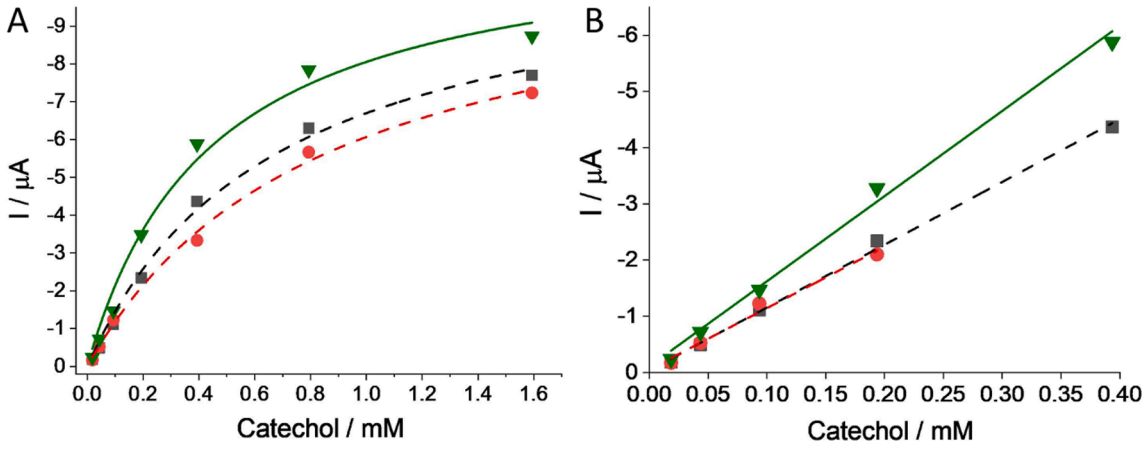

Fig. 5. Typical chronoamperometric calibration curves of bioelectrodes response for substrate saturation (A) and within the linear range (B) toward subsequent addition of increasing catechol concentration. Solid green line – bioelectrode based on $TiO_2S(1.5)$; dash lines – control bioelectrodes: without of TiO_2 (red) and based on commercial AEROXIDE®TiO2 P25 (black).

AgCl was chosen as optimal for further work to study the characteristics of the designed bio-nano-modified electrodes.

The dependence of the operating parameters of Nafion/TiO_2S-modified laccase bioelectrodes on modification of TiO_2S was performed using chronoamperometric analysis (*see supplementary material* Fig. S8). Evaluation of the dependence of the operating parameters of Nafion/TiO_2S-modified laccase bioelectrodes relative to the control (without using TiO_2S) was performed according to four main parameters: I_{max} – the maximal response of the biosensor at substrate saturation; K_M^{app} – the apparent Michaelis-Menten constant; linearity, and sensitivity. The study was performed using nanoparticles of different extents of modification: $TiO_2S(0.75)$; $TiO_2S(1.5)$; $TiO_2S(3.0)$ (with a sulfur content of 2.4 ± 0.2; 6.0 ± 0.3; 12.0 ± 0.8 wt%, respectively). The bioelectrodes based on Nafion membrane without of any TiO_2 nanoparticles and bio-nano-modified electrodes based on commercial nanoparticles (AEROXIDE®TiO2 P25) were used as controls (Figs. 4 and 5).

The main operating parameters are shown in Fig. 4. The control bioelectrodes (without using TiO_2) were characterized by an I_{max} value of 5.16 ± 0.06 μA, K_M^{app} – 0.33 ± 0.02 mM with an upper linearity limit of 0.17 mM toward ABTS, and a sensitivity – 1396 $A{\cdot}M^{-1}{\cdot}m^{-2}$. The bioelectrodes' sensitivity was calculated taking into account that the geometrical surface area of the working electrode was equal to 7.3 mm^2. Compared with the control bioelectrodes (without of TiO_2 nanoparticles), the $TiO_2S(0.75)$-modified bioelectrode was characterized by slightly worse operating parameters: the I_{max} value was 1.6-fold lower (3.17 ± 0.12 μA *vs* 5.16 ± 0.06 μA), and the sensitivity was decreased for 1.7-fold (818 $A{\cdot}M^{-1}{\cdot}m^{-2}$ *vs* 1396 $A{\cdot}M^{-1}{\cdot}m^{-2}$) in contrast to an increased K_M^{app} value for 1.1-fold (0.36 ± 0.05 mM *vs* 0.33 ± 0.02 mM to ABTS) (Fig. 4A). The $TiO_2S(1.5)$-based bioelectrodes showed a significant improvement in the main operating parameters compared to the control bioelectrode: the value of I_{max} was 1.7-fold higher (8.87 ± 0.04 μA *vs* 5.16 ± 0.06 μA for control), the sensitivity increased 2.7-fold (3795 $A{\cdot}M^{-1}{\cdot}m^{-2}$ *vs* 1396 $A{\cdot}M^{-1}{\cdot}m^{-2}$), and its K_M^{app} value was 2.1-fold lower (0.16 ± 0.01 *vs* 0.33 ± 0.02 mM to ABTS for control) (Fig. 4A). The bioelectrodes based on $TiO_2S(3.0)$ with a higher sulfur content (12.0 ± 0.8 wt%) showed significantly worse operating parameters compared to the control bioelectrodes: I_{max} was 5.5-fold lower (0.94 ± 0.03 μA *vs* 5.16 ± 0.06 μA), and the sensitivity was 5.4-fold lower (260 $A{\cdot}M^{-1}{\cdot}m^{-2}$ *vs* 1396 $A{\cdot}M^{-1}{\cdot}m^{-2}$). However, the affinity to ABTS was increased about 1.3-fold (0.26 ± 0.03 mM *vs* 0.33 ± 0.02 mM for ABTS) (Fig. 4B).

For a more detailed characterization of bio-nano-modified electrodes based on TiO_2 with different sulfur content, their operating parameters were compared with a bioelectrode based on a commercial sample of TiO_2 – AEROXIDE®TiO2 P25. The bioelectrode based on AEROXIDE®TiO2 P25 was prepared similarly to the procedure described above. Comparison of the main operational characteristics of the bioelectrodes based on using commercial nanoparticles AEROXIDE®TiO2 P25 with the most promising of the constructed – $TiO_2S(1.5)$-modified bioelectrode, revealed a number of advantages of the latter. The K_M^{app} value was 2.1-fold lower (0.16 ± 0.05 mM *vs* 0.34 ± 0.01 mM), and the sensitivity was increased up to 1.6-fold (3795 $A{\cdot}M^{-1}{\cdot}m^{-2}$ *vs* 2350 $A{\cdot}M^{-1}{\cdot}m^{-2}$ for AEROXIDE®TiO2 P25). However, the bioelectrode, based on $TiO_2S(1.5)$, was characterized by a slightly decreased I_{max} value – 8.87 ± 0.04 μA *vs* 9.32 ± 0.07 μA for AEROXIDE®TiO2 P25 (Fig. 4A).

The increase in the sensitivity of the bio-nano-modified electrode with a simultaneous decrease of K_M^{app} indicates the better electrochemical communication of $TiO_2S(1.5)$ with laccase. Thus, it can be concluded that $TiO_2S(1.5)$-based bioelectrode prevails the bioelectrode formed with commercial AEROXIDE®TiO2 P25 for biosensor application due to better chemical interaction with enzyme. It should be noted that for all of the analyzed bioelectrodes the limit of detection (LOD) and linearity toward ABTS were practically the same (5 μM and linear frames from 0.01 to 0.17 mM, respectively).

For the broader characterization, the best variant of the designed biosensors ($TiO_2S(1.5)$-based) was tested also toward catechol, a typical laccase' substrate and a reference analyte for sensors based on this enzyme. Chronoamperograms of the response of bioelectrodes to the addition of increasing concentrations of catechol are presented in Fig. S9 (*Supplementary material*) and corresponding calibration curves are shown in Fig. 5.

The control bioelectrode (without using TiO_2, Fig. 5) was characterized by an I_{max} value of 11.17 ± 0.7 μA; apparent K_M^{app} – 0.84 ± 0.11 mM, the upper linearity at about 0.2 mM for the catechol, and with a sensitivity of 1382 $A{\cdot}M^{-1}{\cdot}m^{-2}$. The $TiO_2S(1.5)$-based bioelectrode showed a significant improvement of some operational parameters toward catechol compared with the control bioelectrodes: sensitivity was increased 1.5-fold (2075 $A{\cdot}M^{-1}{\cdot}m^{-2}$ *vs* 1382 $A{\cdot}M^{-1}{\cdot}m^{-2}$), and the K_M^{app} value was decreased 1.9-fold (0.44 ± 0.08 mM *vs* 0.84 ± 0.11 mM for control) (Fig. 5). Comparison of the main operational characteristics of the bioelectrodes based on using commercial nanoparticles AEROXIDE®TiO2 P25 and the most promising of our designed bioelectrodes ($TiO_2S(1.5)$-based electrode) demonstrated a number of advantages of the latter in the analysis of catechol. The sensitivity of $TiO_2S(1.5)$-modified bioelectrodes was 1.4-fold higher than AEROXIDE®TiO2 P25-modified (2075 $A{\cdot}M^{-1}{\cdot}m^{-2}$ *vs* 1530 $A{\cdot}M^{-1}{\cdot}m^{-2}$), and the K_M^{app} value was 1.5-fold lower (0.44 ± 0.08 *vs* 0.67 ± 0.08 mM). Both bio-nano-modified electrodes showed practically the same values of the upper linearity range to catechol – 0.4 mM (Fig. 5). The increase in the sensitivity of bio-nano-modified electrodes with a simultaneous

Table 2
Comparison of the main operating parameters of the TiO_2S-based and control bioelectrodes.

Bioelectrode type	I_{max}, μA	K_M^{app}, mM	Upper linear range, mM	Sensitivity, $A{\cdot}M^{-1}{\cdot}m^{-2}$
	ABTS			
Control (without of TiO_2)	5.16 ± 0.06	0.33 ± 0.02	0.17	1396
AEROXIDE®TiO2 P25	9.32 ± 0.07	0.34 ± 0.01	0.17	2350
TiO_2S(0.75)	3.17 ± 0.12	0.36 ± 0.05	0.17	818
TiO_2S(1.5)	8.87 ± 0.04	0.16 ± 0.01	0.17	3795
TiO_2S(3.0)	0.94 ± 0.03	0.26 ± 0.03	0.17	260
	Catechol			
Control (without of TiO_2)	11.18 ± 0.7	0.84 ± 0.11	0.2	1382
AEROXIDE®TiO2 P25	11.15 ± 0.7	0.67 ± 0.08	0.4	1530
TiO_2S(1.5)	11.6 ± 0.8	0.44 ± 0.08	0.4	2075
	Phenol			
TiO_2S(1.5)	7.97 ± 0.35	0.36 ± 0.05	0.4	1168

decrease of the value of apparent K_M^{app}, compared with the control bioelecrodes (without TiO_2 and based on commercial nanoparticles AEROXIDE®TiO2 P25) indicates a better electrochemical communication of TiO_2S(1.5) with laccase.

A summarizing comparison of the main operating parameters of the control bioelectrodes (based on laccase itself without TiO_2), TiO_2S-based bioelectrodes (based on laccase combined with sulfur-doped TiO_2 with different dopant content) and bioelectrodes based on commercial nanoparticles (AEROXIDE®TiO2 P25) toward different laccase substrates is presented in Table 2.

The data, presented in Table 2, testify that the modification of TiO_2 nanoparticles with sulfur with a final content of 6.0 ± 0.3 wt% (TiO_2S(1.5)) significantly improves the operational parameters (sensitivity and K_M^{app}) of the corresponding bio-nano-modified electrode, compared with the control bioelectrodes without TiO_2 or those based on commercial nanoparticles AEROXIDE®TiO2 P25. However, the critical impact of the amount of sulfur in TiO_2S samples for the effective electrical conductivity of the bio-nanocomposite and its good chemical communication with the enzyme should be emphasized. For the TiO_2S(0.75)-based bioelectrode (where the sulfur content was lower and corresponded to 2.4 ± 0.2 wt%), as well as the bioelectrode based on TiO_2S(3.0) (with a high sulfur content – 12.0 ± 0.8 wt%), all operational parameters are significantly worse compared to the control bioelectrodes based on commercial nanoparticles AEROXIDE®TiO2 P25.

The developed TiO_2S(1.5)-modified bioelectrodes were characterized toward phenol also, as the most common pollutant of wastewater (Fig. 6 and *Supplementary material* Fig. S10).

The TiO_2S(1.5)-modified bioelectrodes were characterized by an I_{max} value of 7.97 ± 0.35 μA; K_M^{app} – 0.36 ± 0.05 mM, the upper linearity at about 0.4 mM for the phenol, and with a sensitivity of 1168 $A{\cdot}M^{-1}{\cdot}m^{-2}$ (Fig. 6 and Table 2).

The main operational characteristics of TiO_2S(1.5)-modified bioelectrodes toward catechol as the most common laccase substrate were compared with the recently described analogues (Table 3).

The TiO_2S(1.5)-based biosensor prevails most of the recently published analogues in sensitivity and wider linear frames (Table 3). However, it should be noted that some of the listed biosensors based on the other semiconductors (NiO or MoS_2) demonstrated significantly better sensitivity or wider linearity in comparison to TiO_2S(1.5)-based one [13,14,15]. In the case of NiO it could be explained with their very low size at average 11 nm [14] that supports a high load and better interaction with enzyme molecules. However, the MoS_2 has formed

Table 3
Comparison of the main characteristics of recent nanomaterial-based laccase biosensors for catechol analysis.

Nanocomposition-electrode type	LOD, μM	Linear range, μM	Sensitivity, $\mu A{\cdot}mM^{-1}$	References
NiO/G-SPCE	0.07	1.0 – 100	1500	[13]
NiO/(NCs)-CPE	0.95	2.0 –160	≈ 110	[14]
AuNPs/MoS_2-GCE	2.0	2.0 – 2000	16.3	[15]
CuPcS/AuNPs/CHI-ITO	0.06	2.4 – 17	0.38	[10]
CB-SPCE	2.0	2.5 – 50	≈ 12	[4]
COOH/MWCNT-SPCE	–	0.0 – 0.1	–	[5]
CFs-CRE	5.0	10 – 200	8.3	[6]
M1-CRE	9.9	5.0 – 175	8.6	[33]
TiO_2S(1.5)-CRE	5.0	10 – 400	15.2	Current work

Abbreviations: NiO/G – Ni oxide/graphite; SPCE – screen-printed carbon electrode; NiO/ (NCs) – NiO nanocrystals; CPE – carbon paste electrode; AuNPs/MoS_2 – gold nanoparticles assembled on MoS_2 nanosheets; GCE – glassy carbon electrode; CuPcS/AuNPs/CHI – sulfonated copper phthalocyanine and gold nanoparticles incorporated in chitosan; ITO – indium tin oxide glass electrode; CB – carbon black; COOH/MWCNT – carboxyl functionalized multiwalled carbon nanotubes; CFs – microporous carbon fibers; CRE – carbon rod electrode; M1 – electrochemically polymerized (6,9-bis(4-hexylthiophen-2-yl)-11*H*-indeno [2,1-b]quinoxalin-11-one (M1)); TiO_2S(1.5) – sulfur-doped TiO_2.

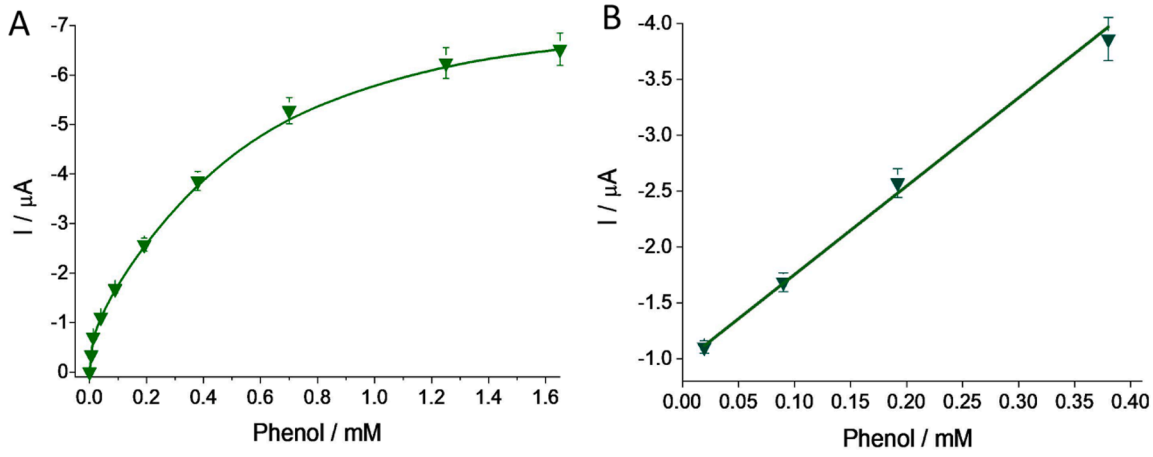

Fig. 6. Chronoamperometric calibration curves of TiO_2S(1.5)-modified bioelectrodes response for substrate saturation (A) and within the linear range (B = 8.53 ± 0.7 $mA{\cdot}mM^{-1}$; R = 0.977) (B) toward subsequent addition of phenol. The results of three replicates of the analysis. Abbreviations: B – slope of the curve; R – correlation coefficient for the linear regression.

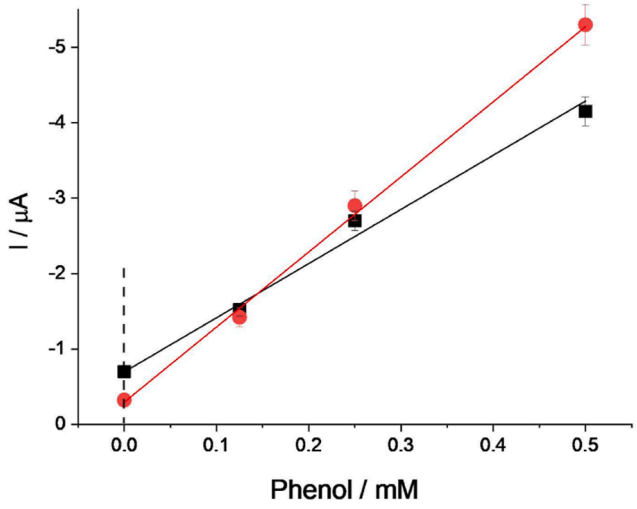

Fig. 7. The calibration curves for biosensor analysis of phenol in the spiked communal wastewater samples using a "standard addition mode"; (red) the sample diluted 40 times ($A = 0.25 \pm 0.09$ μA; $B = 10.1 \pm 0.3$ μA·mM^{-1}; $R = 0.996$; $C_{fin.} = 0.99 \pm 0.02$ mM), (black) the sample diluted 10 times ($A = 0.74 \pm 0.14$ μA; $B = 7.0 \pm 0.5$ μA·mM^{-1}; $R = 0.986$; $C_{fin.} = 1.06 \pm 0.06$ mM). The results of three replicates of the analysis. Abbreviations: A – analyzed sample output; B – slope of the curve; R – correlation coefficient for the linear regression; $C_{fin.}$ – estimated final phenol concentration.

agglomerates with a diameter of about 500 nm [15] that are the same size as TiO_2S(1.5). The MoS_2-based sensor is characterized with comparable sensitivity to TiO_2S(1.5)-based (16.3 *vs* 15.2 μA·mM^{-1}) but fivefold wider linear frames (2000 *vs* 400 μM) (Table 3). The difference between TiO_2S(1.5) and MoS_2 bioelectrodes is the combination of MoS_2 with highly conducting gold nanoparticles. So, it seems that to increase the sensor sensitivity, it should be decreased the TiO_2S(1.5) size, keeping the similar content of sulfur. On the other hand, combination of TiO_2S(1.5) with highly conductive nanomaterials would support increasing the sensor linear frames. These two directions will be advanced in our future investigations.

3.4. Analysis of phenol-spiked real wastewater sample

The developed TiO_2S(1.5)-modified bioelectrodes were used for analysis of phenol in a communal wastewater sample that had been collected at the treatment plant of Lviv (Ukraine) prior to its purification. The wastewater samples were spiked with phenol analytes prior to the analytical experiments with the biosensor electrodes. The spiked samples were made by the addition of 1.0 mM phenol to the raw wastewater. The biosensor analysis was performed using a "standard addition mode" using different dilution steps (10 and 40) of the samples (Fig. 7 and *Supplementary material* Fig. S11).

The biosensor analysis demonstrated the following results for phenol content in the diluted samples (the initial sample was spiked with 1.0 mM phenol): 0.99 ± 0.02 mM for $n = 40$ dilution steps and 1.06 ± 0.06 mM for $n = 10$, respectively (Fig. 7). The calculated average of the tested phenol concentration is equal 1.02 ± 0.04 mM that corresponds to 98% of assay accuracy. This result demonstrates an absence of any interfering impact of the compounds of raw wastewater on biosensor analysis. However, to propose the developed sensor for practical usage, additional testing with respect to the maximum permitted concentration level of phenols in different wastewater should be performed, and this work is in progress.

4. Conclusions

It has been demonstrated that the modification of TiO_2 nanoparticles with sulfur in a final content of 6.0 ± 0.3 wt% (TiO_2S(1.5)) significantly improves the main operational parameters of the corresponding bio-nano-modified electrodes compared with the controls: a bioelectrode without TiO_2 or one based on commercial nanoparticles AEROXIDE®TiO2 P25. The sensitivity of the TiO_2S(1.5)-based bioelectrode toward ABTS was 2.7-fold higher *vs* a control bioelectrode without TiO_2 and 1.6-fold *vs* AEROXIDE®TiO2 P25-modified bioelectrode, as well as for catechol it was higher for 1.5- and 1.4-fold, respectively. The substrate affinity of the TiO_2S(1.5)-based bioelectrode toward ABTS was about 2.1-fold higher compared with both control bio-nano modified electrodes and 1.9–1.5-fold higher for catechol, respectively. The increase in the substrate affinity (decreased value of K_M^{app}) clearly demonstrates their higher bioelectrochemical communication, compared to the other ones, based on the TiO_2S nanoparticles or commercial AEROXIDE®TiO2 P25. Moreover, a significant increase of the sensitivity of the bionanosensor, based on TiO_2S(1.5) nanoparticles, makes it more promising for the analysis of phenolic derivatives in natural groundwater and drinking water, where their concentration is very low. The developed TiO_2S(1.5)-based bioelectrodes were tested for phenol analysis in the real communal wastewater sample spiked with this analyte and demonstrated a high accuracy of the analysis. It has been found that improving the sensor operational parameters for the TiO_2S(1.5)-based laccase electrodes is connected only with impact of sulfur doping but not the difference in the Nafion/TiO_2S-based membrane properties. Taking into account the broad usage of titanium dioxide in practice, including biotechnology and pharmacy [34], it can be predicted that doping of TiO_2 nanoparticles with different dopants is a promising way to obtain new titania-based nanomaterials, maximally fitted for construction of biosensors.

Declaration of Competing Interest

The authors declare that they have no known competing financial interests or personal relationships that could have appeared to influence the work reported in this paper.

Acknowledgements

This work was supported in part by the Ministry of Education and Science of Ukraine (projects Nos. 0118U000297, 0119U100671, 0120U102224, 0120U103398, 0121U109539, 0121U109543, 0122U000850, and 0122U000874), National Academy of Sciences of Ukraine in the framework of the Scientific-Technical Program "Smart sensor devices of a new generation based on modern materials and technologies" (projects Nos. 13 and 10/3), National Research Foundation of Ukraine (projects Nos. 2020.02/0100 "Development of new nanozymes as catalytic elements for enzymatic kits and chemo/biosensors" and 2021.01/0010 "Development of an enzymatic kit and portable biosensors for express-analysis of creatinine, a marker of acute functional disorders of the kidneys"), JSPS KAKENHI (Grant Nos. 17 K05123 and 20 K12506), collaboration research project of Integrated Radiation and Nuclear Science, Kyoto University (No. R2104), Slovak Grant Agency VEGA (projects Nos. 2/0029/20 and 2/0134/21), and Slovak Research and Development Agency (projects Nos. APVV-16-0369 and APVV-21-0335). T.K. and Yu.K. also acknowledge the SAIA (Slovak Academic Information Agency) for scholarships in the IPSAS in the framework of the National Scholarship Programme of the Slovak Republic.

Appendix A. Supplementary material

Supplementary data to this article can be found online at https://doi.org/10.1016/j.bioelechem.2022.108215.

References

[1] V. Naresh, N. Lee, A review on biosensors and recent development of nanostructured materials-enabled biosensors, Sensors 21 (2021) 1109, https://doi.org/10.3390/s21041109.

[2] L. Fritea, F. Banica, T.O. Costea, L. Moldovan, L. Dobjanschi, M. Muresan, S. Cavalu, Metal nanoparticles and carbon-based nanomaterials for improved performances of electrochemical (bio)sensors with biomedical applications, Materials 14 (2021) 6319, https://doi.org/10.3390/ma14216319.

[3] N. Stasyuk, O. Smutok, O. Demkiv, T. Prokopiv, G. Gayda, M. Nisnevitch, M. Gonchar, Synthesis, catalytic properties and application in biosensorics of nanozymes and electronanocatalysts: a review, Sensors 20 (2020) 4509, https://doi.org/10.3390/s20164509.

[4] M.C. Castrovilli, P. Bolognesi, J. Chiarinelli, L. Avaldi, A. Cartoni, P. Calandra, E. Tempesta, M.T. Giardi, A. Antonacci, F. Arduini, V. Scognamiglio, Electrospray deposition as a smart technique for laccase immobilisation on carbon black-nanomodified screen-printed electrodes, Biosens. Bioelectron. 163 (2020), 112299, https://doi.org/10.1016/j.bios.2020.112299.

[5] A.M. Othman, U. Wollenberger, Amperometric biosensor based on coupling aminated laccase to functionalized carbon nanotubes for phenolics detection, Int. J. Biol. Macromol. 153 (2020) 855–864, https://doi.org/10.1016/j.ijbiomac.2020.03.049.

[6] T. Kavetskyy, O. Smutok, O. Demkiv, I. Maťko, H. Švajdlenková, O. Šauša, I. Novák, D. Berek, K. Čechová, M. Pecz, O. Nykolaishyn-Dytso, R. Wojnarowska-Nowak, D. Broda, M. Gonchar, B. Zgardzińska, Microporous carbon fibers as electroconductive immobilization matrixes: Effect of their structure on operational parameters of laccase-based amperometric biosensor, Mater. Sci. Eng. C. 109 (2020), 110570, https://doi.org/10.1016/j.msec.2019.110570.

[7] O. Smutok, T. Kavetskyy, T. Prokopiv, R. Serkiz, R. Wojnarowska-Nowak, O. Šauša, I. Novák, D. Berek, A. Melman, M. Gonchar, New micro/nanocomposite with peroxidase-like activity in construction of oxidases-based amperometric biosensors for ethanol and glucose analysis, Anal. Chim. Acta 1143 (2021) 201–209, https://doi.org/10.1016/j.aca.2020.11.052.

[8] C. Lou, T. Jing, J. Tian, Y. Zheng, J. Zhang, M. Dong, C. Wang, C. Hou, J. Fan, Z. Guo, 3-Dimensional graphene/Cu/Fe3O4 composites: Immobilized laccase electrodes for detecting bisphenol A, J. Mater. Res. 34 (2019) 2964–2975, https://doi.org/10.1557/jmr.2019.248.

[9] I. Almeida, F. Henriques, M. Carvalho, A. Viana, Carbon disulfide mediated self-assembly of Laccase and iron oxide nanoparticles on gold surfaces for biosensing applications, J. Colloid Interface Sci. 485 (2017) 242–250, https://doi.org/10.1016/j.jcis.2016.09.042.

[10] C. Salvo-Comino, A. González-Gil, J. Rodriguez-Valentin, C. Garcia-Hernandez, F. Martin-Pedrosa, C. Garcia-Cabezon, M.L. Rodriguez-Mendez, Biosensors platform based on chitosan/AuNPs/phthalocyanine composite films for the electrochemical detection of catechol. The role of the surface structure, Sensors (Basel) 20 (2020) 2152, https://doi.org/10.3390/s20072152.

[11] T. Kavetskyy, N. Stasyuk, O. Smutok, O. Demkiv, Y. Kukhazh, N. Hoivanovych, V. Boev, V. Ilcheva, T. Petkova, M. Gonchar, Improvement of amperometric laccase biosensor using enzyme-immobilized gold nanoparticles coupling with ureasil polymer as a host matrix, Gold Bull. 52 (2019) 79–85, https://doi.org/10.1007/s13404-019-00255-z.

[12] I. Serban, A. Enesca, Metal oxides-based semiconductors for biosensors applications, Front. Chem. 8 (2020) 354, https://doi.org/10.3389/fchem.2020.00354.

[13] R. Pillai, S. Preetha, B. Narasimhamurthy, I.C. Lekshmi, Biosensing of catechol via amperometry using laccase immobilized nickel oxide/graphite modified screen-printed electrodes, Mater. Today: Proc. 62 (2022) 5434–5438, https://doi.org/10.1016/j.matpr.2022.03.708.

[14] I.C. Lekshmi, I. Rudra, R. Pillai, C. Sarika, M.S. Shivakumar, C. Shivakumara, S. B. Konwar, B. Narasimhamurthy, Enhanced catechol biosensing on metal oxide nanocrystal sensitized graphite nanoelectrodes through preferential molecular adsorption, J. Electroanal. Chem. 867 (2020), 114190, https://doi.org/10.1016/j.jelechem.2020.114190.

[15] Y. Zhang, X. Li, D. Li, Q. Wei, A laccase based biosensor on AuNPs-MoS2 modified glassy carbon electrode for catechol detection, Colloids Surf. B: Biointerfaces 186 (2020), 110683, https://doi.org/10.1016/j.colsurfb.2019.110683.

[16] A.S. Agnihotri, A. Varghese, M. Nidhin, Transition metal oxides in electrochemical and bio sensing: A state-of-art review, Applied Surface Science Advances 4 (2021), https://doi.org/10.1016/j.apsadv.2021.100072.

[17] J. Bai, B. Shou, Titanium dioxide nanomaterials for sensor applications, Chem. Rev. 114 (2014) 10131–10176, https://doi.org/10.1021/cr400625j.

[18] M. Romero-Arcos, M.G. Garnica-Romo, H.E. Martínez-Flores, Electrochemical study and characterization of an amperometric biosensor based on the immobilization of laccase in a nanostructure of TiO2 synthesized by the sol-gel method, Materials (Basel) 9 (2016) 543, https://doi.org/10.3390/ma9070543.

[19] D. Thomaz, G. Brazil, Development of laccase-TiO_2@carbon paste biosensor for voltammetric determination of paracetamol, Int. J. Electrochem. Sci. 13 (2018) 10884–10893, https://doi.org/10.20964/2018.11.61.

[20] A. Klumpp, A. Adrovic, J. Boudaden, Enzymatic sensor based on dye sensitized TiO2 electrode for detection of catechol in water, Proceedings 2 (2018), 737, https://doi.org/10.3390/proceedings2130737.

[21] A.A. Kadam, G.D. Saratale, G.S. Ghodake, R.G. Saratale, A. Shahzad, V.K. Magotra, M. Kumar, R.R. Palem, J.-S. Sung, Recent advances in the development of laccase-based biosensors via nano-immobilization techniques, Chemosensors 10 (2022) 58, https://doi.org/10.3390/chemosensors10020058.

[22] G.M. Telbiz, V.N. Vlasenko, O.Z. Didenko, P.E. Strizhak, Acid-base and catalytic properties of sulfated mesoporous titanium oxide in glycerol oligomerization, Theor. Exp. Chem. 13 (2020) 199–204, https://doi.org/10.1007/s11237-020-09652-4.

[23] Y. Wang, Z.H. Chen, Bioinformatics and enzymatics investigation of Trametes laccase for optical biosensing application, J. Mater. Sci. 54 (2019) 4970–4983, https://doi.org/10.1007/s10853-018-03187-9.

[24] A. Larbot, I. Laaziz, J. Marignan, J.F. Quinson, Porous texture of a titanium oxide gel: evolution as a function of medium used, J. Non-Cryst. Solids 147–148 (1992) 157–161, https://doi.org/10.1016/S0022-3093(05)80610-6.

[25] M. Nakajima, R. Taguchi, A. Yabuuchi, A. Kinomura, Reduction of background radiation effects for positron lifetime measurements in the slow positron beamline at the Kyoto University Research Reactor, Rev. Sci. Instrum. 91 (2020) 125109, https://doi.org/10.1063/1.1677067.

[26] X. Deng, Z. Ma, Y. Yue, Z. Gao, Catalytic hydrolysis of dichlorodifluoromethane over nanosized titania-supported titanyl sulfate, J. Catal. 204 (2001) 200–208, https://doi.org/10.1006/jcat.2001.3392.

[27] S.J. Tao, Positronium annihilation in molecular substances, J. Chem. Phys. 56 (1972) 5499–5510, https://doi.org/10.1063/1.1677067.

[28] M. Eldrup, D. Lightbody, J.N. Sherwood, The temperature dependence of positron lifetimes in solid pivalic acid, Chem. Phys. 63 (1981) 51–58, https://doi.org/10.1016/0301-0104(81)80307-2.

[29] H. Nakanishi, Y.Y. Wang, Y.C. Jean, In: Positron Annihilation Studies of Fluids, edited by S.C. Sharma, World Scientific: Singapore, 1988, p. 292.

[30] H. Murakami, N. Onizuka, J. Sasaki, N. Thonghai, Ultra-fine particles of amorphous TiO2 studied by means of positron annihilation spectroscopy, J. Mater. Sci. 33 (1998) 5811–5814, https://doi.org/10.1023/A:1004450015173.

[31] Y.F. Li, Z.M. Liu, Y.L. Liu, Y.H. Yang, G.L. Shen, R.Q. Yu, A mediator-free phenol biosensor based on immobilizing tyrosinase to ZnO nanoparticles, Anal. Biochem. 349 (2006) 33–40, https://doi.org/10.1016/j.ab.2005.11.017.

[32] X.H. HuiqinLi, H. Zhu, Y. Zang, H. Xue, Amperometric phenol biosensor based on a new immobilization matrix: polypyrrole nanotubes derived from methyl orange as dopant, Int. J. Electrochem. Sci 12 (2017) 6714–6728.

[33] Ş.C. Cevher, S.A. Bekmezci, S. Soylemez, Y.A. Udum, L. Toppare, A. Çırpan, Indenoquinoxalinone based conjugated polymer substrate for laccase biosensor, Mater. Chem. Phys. 257 (2021), 123788, https://doi.org/10.1016/j.matchemphys.2020.123788.

[34] D. Ziental, B. Czarczynska-Goslinska, D.T. Mlynarczyk, A. Glowacka-Sobotta, B. Stanisz, T. GoslinskiGoslinski, L. Sobotta, Titanium dioxide nanoparticles: prospects and applications in medicine, Nanomaterials (Basel) 10 (2020) 387, https://doi.org/10.3390/nano10020387.